J. Astrophys. Astr. (2019) 40:17
https://doi.org/10.1007/s12036-019-9585-2

Study of diffuse emission in cluster MACSJ0417.5-1154 from 76 MHz to 18 GHz

PRITPAL SANDHU[1], RAMIJ RAJA[1,*], MAJIDUL RAHAMAN[1], SIDDHARTH MALU[1] and ABHIRUP DATTA[1,2]

[1]Centre of Astronomy, Indian Institute of Technology Indore, Simrol, Khandwa Road, Indore 453 552, India.
[2]Center for Astrophysics and Space Astronomy, Department of Astrophysical Planetary Science, University of Colorado, Boulder, CO 80309, USA.
*Corresponding author. E-mail: phd1601121008@iiti.ac.in

MS received 5 October 2018; accepted 11 March 2019; published online 5 April 2019

Abstract. We present new radio observations of the massive and X-ray luminous galaxy cluster MACS J0417.5–1154, at 1.387 GHz and 18 GHz, from the Giant Metrewave Radio Telescope (GMRT) and the Australia Telescope Compact Array (ATCA) respectively. We estimate diffuse emission in the central region of the cluster at 1.387 GHz and 18 GHz. We combine these data with previously published results and present the spectrum of diffuse emission from 76 MHz to 18 GHz. This is possibly a unique study of the radio halo emission in galaxy cluster over this wide range of frequencies. Such studies lay the prospects of future studies with radio telescopes with wide-range of frequencies like the Square Kilometre Array (SKA). Our 1.387 GHz data, with 2″ angular resolution, provides a better estimate of point source emission than previous L-band observations, which is crucial, given the claim of sharp steepening of the radio halo spectrum at 0.61 GHz reported earlier. We find that the spectrum of the radio halo has a spectral index fit up to 18 GHz, and yields a spectral index between 76 MHz and 18 GHz that fits the available data better than earlier L-band observations. We discuss possible reasons for the peculiar spectral characteristics of the diffuse emission.

Keywords. Galaxies—clusters—individual (MACS J0417.5-1154)—intergalactic medium—radio continuum—general—techniques—interferometric.

1. Introduction

Clusters of galaxies are the largest gravitationally bound systems in the universe and are ideal laboratories to study the formation and evolution of cosmic structure. The tenuous diffuse gaseous component of galaxy clusters, known as Intra Cluster Medium (ICM), emits in soft X-ray via thermal bremsstrahlung, the detection of which has advanced our understanding of galaxy clusters only recently (Feretti *et al.* 2012; Brunetti and Jones 2014). Non-thermal emission in radio band from ICM confirms the presence of cluster-wide magnetic field. The diffuse radio sources, 'Radio Halos' and 'Radio Relics' depending upon their physical location in the cluster, are believed to be present only in mergers, although not all merging cluster host them (Brunetti *et al.* 2009; Venturi *et al.* 2008).

Observations of diffuse emission from cluster mergers have yielded information about the dynamical state of clusters, and their magnetic fields (see, e.g., Brunetti and Jones 2014 for a review). It is known that a re-acceleration mechanism is required that can inject sufficient energy into the non-thermal plasma in clusters, in order to generate giant radio halos. Mergers between galaxy clusters is one process that can provide the energy required for the re-acceleration of relativistic electrons (Brunetti *et al.* 2001; Petrosian 2001). Another process involves protons and ions in the ICM, which leads to the production of secondary electrons (Dennison 1980; Blasi and Colafrancesco 1999). Since these protons diffuse throughout the cluster medium, they can continuously produce secondary electrons, which emit synchrotron radiation (Brunetti and Jones 2014). For these two models, the expected spectral behaviour is different – spectra from the secondary electron model are expected to be flatter than in the re-acceleration model. Additionally, spectral steepening is expected in the re-acceleration model, with the frequency of spectral

Table 1. Summary of the GMRT and ATCA observations.

Array	Frequency (GHz)	Observing time (hours)	Date
GMRT	1.387	7.5	2014 June 14
		7.9	2014 June 15
		3.8	2014 June 17
		9.2	2014 Sept 14
		9.0	2014 Sept 15
ATCA	18.0	8.0	2011 Oct 11

steepening depending on the energy involved in the cluster merger. Therefore, spectra of diffuse emission from giant radio halos are required over a large frequency range, in order to be able to differentiate between these models of radio halo formation.

MACSJ0417.5-1154 at $z = 0.443$ is one of the 34 X-ray brightest clusters catalogued in MAssive Cluster Survey (MACS) in the redshift range 0.3 to 0.5 (Ebeling *et al.* 2010). This highly X-ray luminous ($\sim 10^{45}$ erg s^{-1}) and massive (12.25×10^{14} $M_\odot$) cluster has a disturbed X-ray morphology, which implies the possibility of merger. The first detection of a Giant Radio Halo in this cluster was reported by Dwarakanath *et al.* (2011) at 235 and 610 MHz and has an elongated structure similar to that observed in X-ray. Further radio observations of this cluster have been reported by Parekh *et al.* (2017) at 1575 MHz (EVLA observations), and 5.5 and 9 GHz ATCA observations as described in Sandhu *et al.* (2018). Our work extends the observed spectrum further to 18 GHz and reinvestigates the radio emission at L-band with 1387 MHz GMRT observations.

We describe our radio observations in Section 2.1 and Section 2.2, diffuse emission estimation and analysis in Section 2.3, and discuss possible reasons for the peculiar nature of diffuse emission in this cluster in Section 3 Throughout the paper we adopt a ΛCDM cosmology with $H_0 = 70\,\mathrm{km\,s^{-1}\,Mpc^{-1}}$, $\Omega_m = 0.27$, and $\Omega_\Lambda = 0.73$ (Table 1).

2. Radio observations and data reduction

2.1 *L-Band GMRT data*

MACSJ0417.5−1154 was observed with GMRT (Giant Metrewave Radio Telescope) for 37.4 hours at 1387 MHz. Full stokes observations were done with 256 channels over 32 MHz bandwidth with integration time 16 sec. Data analysis was done using SPAM (Source Peeling and Atmospheric Modeling) developed by Intema *et al.* (2009). The data were inspected for RFI (Radio Frequency Interference) and other issues and excised. The flux density of the flux calibrator was set according to the Scaife and Heald (2012). Data reduction was performed following the standard procedure of bandpass and gain calibration. Several rounds of self-calibration was performed in the pipeline to further refine the data. Direction dependent calibration was not performed due to too few peeled sources. From the calibrated data imaging was done by standard Fourier transform deconvolution method using CASA task 'clean'. Imaging was done with multi-frequency synthesis along with wide-field imaging (using 512 w-projection planes). For low resolution image we used a maximum uvrange of 11 kilolambda with tapering of 3.85 kilolambda and robust parameter 0.5 of Briggs weighting scheme. The image (Figure 1) was convolved with $20'' \times 20''$ beam, in order to keep our resolution same as that of Parekh *et al.* (2017) results at L-band. It should be noted that Parekh *et al.* (2017) used this restoring beam size in order to match the TIFR GMRT Sky Survey (TGSS) (Intema *et al.* 2017) beam to estimate the spectral index in between those frequencies. The off-source rms noise near the centre of the image is 50 μJy/beam. We found the largest linear size (LLS) of the diffuse emission at this frequency of 0.91 Mpc (angular size $\sim 157.3''$).

2.1.1 A comparison of L-band images from GMRT (1.387 GHz, current work) and EVLA (1.575 GHz, Parekh et al. (2017)) One of the main differences between the 1.387 GHz GMRT image presented in this paper and the 1.575 GHz EVLA image (Parekh *et al.* 2017) is the resolution attained. The best resolution in the GMRT data is $\sim 2''$ using Briggs robust parameter −1, whereas the 1.575 GHz EVLA image has a resolution of $20''$, as shown in Fig. 1 in Parekh *et al.* (2017). With our significantly better resolution of $2''$, it is possible to discern structure in the sources that are reported

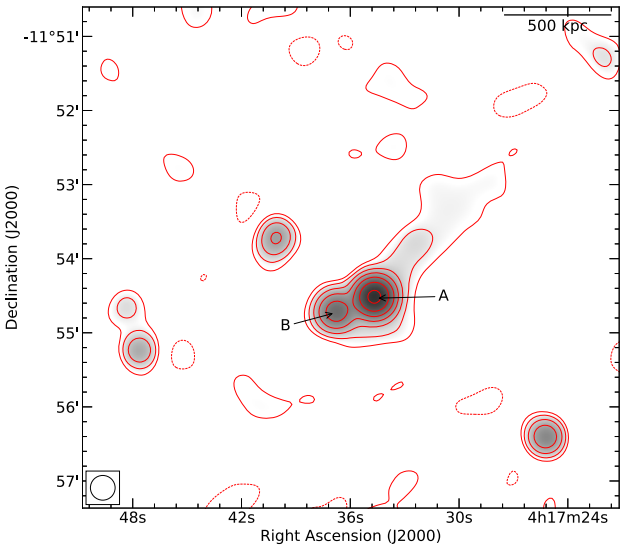

Figure 1. The GMRT radio image of the Galaxy cluster at 1387 MHz. The resolution of this image is 20″ with rms noise of 50μJy/beam. The contours levels are drawn at [1, 2, 4, 8, ...] × 3σ. Dashed lines are negative contours at 3σ.

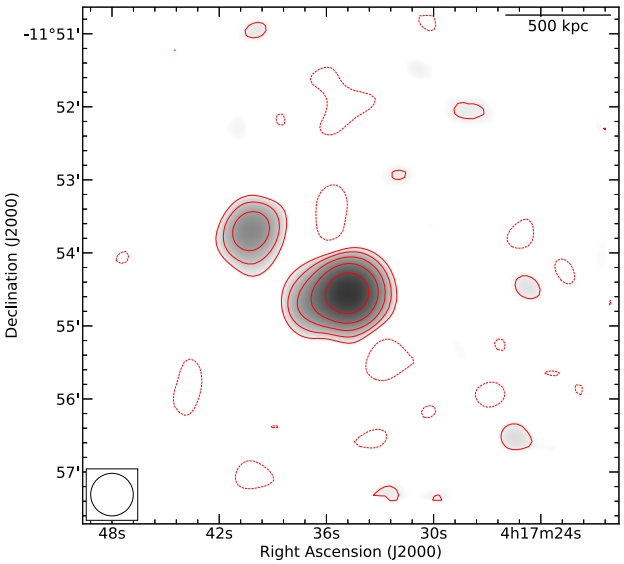

Figure 2. The ATCA radio image of the Galaxy cluster at 18 GHz. The resolution of this image is 35″ with rms noise (σ) of 8μJy/beam. The contours levels are drawn at [1, 2, 4, 8, ...] × 5σ. Dashed lines are negative contours at 3σ.

as unresolved in Parekh *et al.* (2017). Since the noise rms obtained for the high resolution image is better (30μJy beam^{-1} for our 1.387 GHz GMRT observations, and 40μJy beam^{-1} for the 1.575 GHz EVLA observations reported in Parekh *et al.* 2017), this has enabled a more accurate estimate of the point-source flux, and as a result, a more accurate estimate of the integrated flux of the diffuse emission in the central region. As presented in Fig. 4 of Sandhu *et al.* (2018), the fluxes of the two sources A and B (labels from Parekh *et al.* 2017) are 11.66 ± 0.12 mJy and 3.75 ± 0.17 mJy respectively. Parekh *et al.* (2017) report 13 ± 1.3 mJy and 4 ± 0.4 mJy respectively for the sources A and B.

2.2 *18 GHz ATCA data*

MACSJ0417.5−1154 was observed for 8 hours with ATCA (Australia Telescope Compact Array) H75 array, the most compact array configuration, and the upgraded Compact Array Broadband Backend (CABB; Wilson *et al.* 2011). Observations were done in full stokes mode with 2048 channels of width 1 MHz with central frequencies of the two bands at 17 and 19 GHz. Bad data were searched and excised. Both bands were calibrated separately using 1934−638 as primary/amplitude calibrator and 0403−132 as secondary/phase calibrator. Data reduction was done using the package Multichannel Image Reconstruction, Image Analysis and Display (MIRIAD). Standard calibration method was followed in calibrating primary and secondary calibrators, followed by the application of the calibration tables on the target data. After averaging visibilities over a 5-minute interval, data having in excess of 4 times the standard deviation in amplitude were excised to get rid of any remaining interference. Calibrated data of both band centered at 17 and 19 GHz were used to make a combined image. MIRIAD task 'invert' was used to transform mosaicked visibility data into a map followed by 'mossdi' to perform a steer CLEAN on the mosaicked image. To restore the clean components and make the CLEAN map task 'restor' was used. The image (Figure 2) was convolved with 35″ × 35″ beam which is the maximum resolution achievable with the current data. Stokes-V does not contain signal and was therefore used to estimate the rms noise in the image which was found to be 8μJy/beam. Natural weighting scheme was used. The uv-coverage of the data was 1.6 kilolambda to 6.0 kilolambda. We found the largest linear size (LLS) of the diffuse emission at this frequency of 0.56 Mpc (angular size ∼ 98″).

2.3 *Diffuse emission estimation at 1.387 and 18 GHz and analysis*

To estimate the amount of diffuse emission present in the halo region at 1.387 GHz we have used the approach taken by Parekh *et al.* (2017), and subsequently by Sandhu *et al.* (2018). First, we estimated the total flux inside the 3σ contour

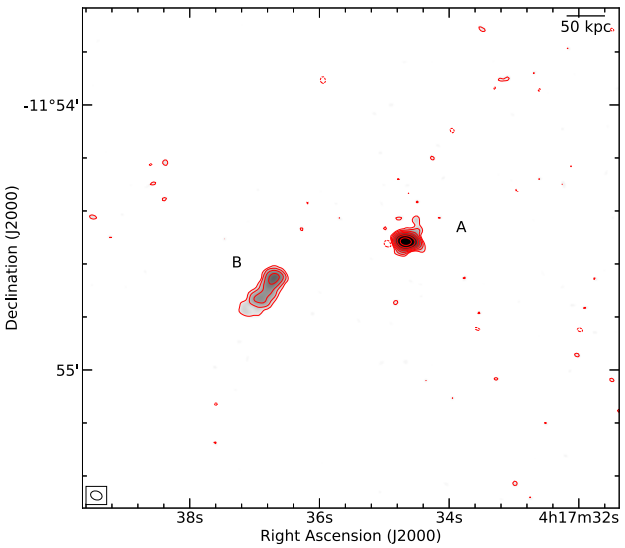

Figure 3. The GMRT radio image of the Galaxy cluster at 1387 MHz. The resolution of this image is 2″ with rms noise of 30μJy/beam. The contours levels are drawn at [1, 2, 4, 8, ...] × 3σ. Dashed lines are negative contours at 3σ.

Table 2. Flux density of the point sources.

Frequency (GHz)	Flux Density (mJy) Source A	Flux Density (mJy) Source B
1.387	11.66 ± 0.12	3.75 ± 0.17
18	0.77 ± 0.07*	0.36 ± 0.04*

* These are calculated by extrapolating the 5.5–9 GHz spectrum of the point sources A and B to 18 GHz

(Figure 1) in the cluster region. Then, from the high resolution image with the best resolution at 1.387 GHz (2″, Figure 3) the flux densities of the two point sources were estimated using gaussian fitting method (Table 2) using PyBDSF (Python Blob Detection and Source Finder) developed by Mohan *et al.* (2015). Finally, the fluxes of these two point sources were subtracted from the estimated total integrated flux in the cluster region. The above method makes no assumption about the spectral index of the point sources, or the diffuse emission, and has ensured the use of high-resolution data from the same observation. Our estimates of the point source flux densities in L-band are more accurate than those reported by Parekh *et al.* (2017) and are consistent also. The apparent discrepancy in the Halo flux is because of the sparse coverage of the shorter baselines in the GMRT observation. So, our observation confirms that the Halo emission at 1.575 GHz was fairly estimated.

Since the resolution of the 18 GHz image was not adequate to separately estimate the flux densities of point sources A and B, we adopted the following approach. For each of these sources, we adopted the spectral index between 5.5 GHz and 9 GHz from the point source flux estimates in Sandhu *et al.* (2018). These were found to be −1.65 and −0.94 for the sources A and B respectively. Then, the fluxes calculated for these two point sources at 18 GHz were subtracted from the total emission estimated inside the 3σ contour level (Figure 2) in the cluster region.

The integrated flux density of the radio halo region of MACSJ0417.5−1154 at different frequencies are listed in Table 3. The spectrum of the radio halo region is presented in Figure 4. We have used different combinations of data points to derive spectral indices at several parts of the total bandwidth 76 MHz and 18 GHz, as given below (see Table 3 for source of the data points).

The accuracy of estimation of cluster-wide diffuse emission depends on

1. Large angular scales (∼0.3-1 arcmin) being imaged, so that diffuse emission across the entire cluster is imaged
2. Small angular scales (∼2-5 arcsec) being imaged, so that point source fluxes can be estimated accurately

In other words, good uv-coverage across a wide uv-range is required.

If there is a lack of uv-coverage at large angular scales (but with good uv-coverage at small angular scales), diffuse emission flux may be underestimated. If there is a lack of uv-coverage at small angular scales (but with good uv-coverage at large angular scales), diffuse emission flux may be overestimated.

Now, if the same radio interferometer array is used to image diffuse emission across frequencies, then clearly, at the higher frequencies, uv-coverage at large angular scales would be poor compared to lower frequencies, resulting in lower estimates of diffuse emission at higher frequencies. This may lead to the estimated spectra appearing steeper. This may be the case for the 5.5 GHz and 9 GHz diffuse emission estimates reported earlier in Sandhu *et al.* (2018).

3. Discussion and summary

We have presented radio observations of the galaxy cluster MACS J0417.5-1154 at 1.387 and 18 GHz (obtained using GMRT and ATCA respectively), and

Table 3. Integrated Flux density of the Radio Halo region.

Label	Frequency (GHz)	Flux Density (mJy)	Ref.	Resolution (arcsec)
o	0.076	$615 \pm 44^{\oplus}$	2	296×281
a	0.150	$250 \pm 90^{\dagger}$	2	159×150
b	0.235	$108 \pm 10^{\oplus}$	2	109×105
c	0.235	77 ± 8	3	20×20
d	0.610	50 ± 5.5	3	20×20
e	1.387	4.9 ± 0.23	1	20×20
f	1.575	10.6 ± 1	3	20×20
g	5.5	1.23 ± 0.11	2	46.3×31.9
h	9.0	0.51 ± 0.11	2	46.3×31.9
i	18.0	0.2 ± 0.05	1	35×35

$^{\oplus}$ GLEAM (GaLactic and Extragalactic All-sky MWA) survey (Hurley-Walker *et al.* 2017) data
† GLEAM data at 150 MHz was used, and TGSS data was used to subtract point sources at 150 MHz
(1) Current work
(2) Sandhu *et al.* (2018)
(3) Parekh *et al.* (2017)

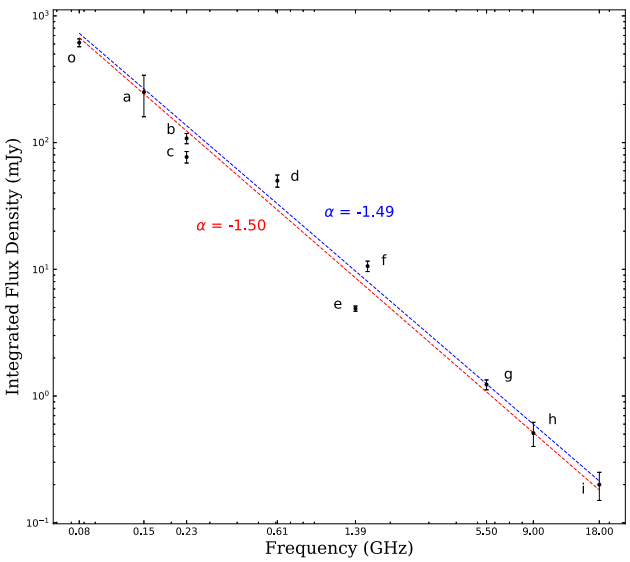

Figure 4. The spectrum of diffuse radio emission in MACSJ0417.5-1154 for data ranging from 76 MHz to 18 GHz. Single spectral index fit using data point (f) (in blue) is $\alpha = -1.49$ with reduced χ^2 of 5.75 and using data point (e) (in red) is $\alpha = -1.50$ with reduced χ^2 of 3.90 respectively.

the spectrum of diffuse emission in the central region of the cluster, from 0.076 to 18 GHz. This is a very massive and the second most X-ray luminous cluster in the MACSurvey (Ebeling *et al.* 2010). We have presented here a single spectral index fit for the entire radio data available (76 MHz to 18 GHz; Figure 4). We have shown two single spectral fit corresponding to two L-band observations. It is evident that a single spectral index fit with $\alpha \sim -1.5$ fits all the data points well. We have tested goodness of fit with the χ^2 test. The linear model with the spectral index of -1.49 (blue) uses the Halo flux at 1.575 GHz (Parekh *et al.* 2017) and has a reduced χ^2 of 5.75 whereas using our data point at 1.387 GHz, we get $\alpha = -1.50$ (red) with a reduced χ^2 of 3.90 which indicates a fairly good fit across such wide range of frequencies.

Our discovery of diffuse emission in the central region of this cluster at 18 GHz provides another puzzle for this peculiar cluster. The north-west elongation in the diffuse emission at 18 GHz is missing, as in the 9 GHz data in Sandhu *et al.* (2018). Interestingly, our 1.387 and 18 GHz data ensure that the spectral index between 0.61 and 18 GHz matches with the estimates provided in Parekh *et al.* (2017) and Sandhu *et al.* (2018).

We found non-trivial structure of the point sources embedded in the halo region. Therefore, it is not clear how much contribution these point sources make in the diffuse emission estimation, and simple Gaussian fitting of these point sources may not provide reliable estimates of diffuse emission. However, we did estimate flux density of these point sources (A and B) with multiple gaussian fitting and found these to be consistent with previously reported values by Parekh *et al.* (2017). High resolution images are needed at several radio frequencies for better understanding of these sources, in order

to obtain better estimates of diffuse emission. We point out the fact that our estimation of point-source fluxes are more accurate, due to the high-resolution data available at 1.387 GHz in the current work, and 5.5 GHz and 9 GHz in earlier work (Sandhu *et al.* 2018).

According to Parekh *et al.* (2017), ~ 1 Gyr has passed since merger and turbulence has decayed and due to less efficient re-acceleration the kink in the spectrum has shifted to < 1 GHz frequency. Brown *et al.* (2011) discuss two scenarios for clusters with sub-luminous diffuse emission at GHz frequencies. They state that high L_X and disturbed X-ray morphology clusters can exist in an 'off' state; these clusters may exhibit some Mpc-scale diffuse emission at low radio frequencies (i.e. below 1.4 GHz), but at GHz frequencies are sub-luminous. For such clusters, one scenario according to Brown *et al.* (2011) is that the cluster merger with which the diffuse emission is associated may be less energetic – this can give rise to extremely steep spectra of diffuse emission. In the other scenario, cosmic ray (CR) protons and their secondary products CR electrons are re-accelerated by magnetohydrodynamic turbulence, and synchrotron emission scales with turbulence – in such systems, radio halos gradually gain luminosity with time, as the ICM becomes increasingly turbulent. However, since a single spectral index fits all the data points suggest that there may not be any break at all.

A third possibility, also mentioned by Brown *et al.* (2011), is that of a non-thermal population of electrons in the cluster core due to the presence of radio galaxies/AGNs and their jets. This is relevant in the present case, since one of the sources in the central regions of this cluster exhibit non-trivial structure, which may well be part of radio galaxy jets. It is possible that a portion of the diffuse emission in the central region of this cluster is due to turbulent re-acceleration of this non-thermal plasma.

A recent study by Sandhu *et al.* (2018) of this cluster has pointed out the possibility of the diffuse emission being underestimated at 235 MHz – this implies that the spectral cutoff may not be as sharp as it seems, as pointed out by them. In that case, the spectral cutoff or turnover may not occur, i.e. the data is consistent with a single spectral index. This fact makes way for yet another interpretation of the merger age to be recent. Hence, there is no break in the spectrum. Here, we have tried to investigate whether there is a higher frequency cut-off in the spectrum. We used our 18 GHz observation on the same cluster to do the same. But we could not find any evidence of such a break.

Skillman *et al.* (2013) have pointed out that peak X-ray emission precedes peak radio emission by 0.2–0.5 Gyr. In addition, absence of any radio relic also points to the lack of radio emission in the cluster. The combination of these two facts points to the cluster merger being recent, which is exactly the conclusion we reached above. Thus, the lack of radio emission in this cluster is consistent with the merger being too recent to be detectable in radio.

In conclusion, we have presented for the first time the spectrum of the diffuse radio emission in the cluster MACS J0417.5−1154 for a wide range of frequencies spanning from 76 MHz to 18 GHz. A single spectral index fits the data well upto 18 GHz supporting the previous studies done by Sandhu *et al.* (2018) and also rules out the significance of a possible spectral break at 610 MHz. However, it should be iterated that the current status of radio observations are not conclusive. The need for better angular resolution along with sufficient uv-coverage is required to reveal the cluster radio halo properties with adequate confidence. Importance of upcoming telescopes like the MeerKAT and the SKA (Square Kilometre Array) is very critical in this regard.

Acknowledgements

We thank the staff of the GMRT and ATCA who have made these observations possible. GMRT is run by the National Centre for Radio Astrophysics of the Tata Institute of Fundamental Research. ATCA is part of the Australia Telescope which is funded by the Commonwealth of Australia for operation as a National Facility managed by CSIRO. We thank Nirupam Roy for discussion and suggestions in the L-Band GMRT data reduction. Analysis of radio data was made possible by a generous grant for Astronomy by IIT Indore.

References

Blasi P., Colafrancesco S. 1999, APh, 12, 169
Brown S., Emerick A., Rudnick L., Brunetti G. 2011, ApJ, 740, L28
Brunetti G., Setti G., Feretti L., Giovannini G. 2001, MNRAS, 320, 365
Brunetti G., Jones T. W. 2014, IJMPD, 23, 1430007-98
Brunetti G., Cassano R., Dolag K., Setti G. 2009, A&A, 507, 661
Dennison B. 1980, ApJ, 239, L93
Dwarakanath K. S., Malu S., Kale R. 2011, JApA, 32, 529
Ebeling H., Edge A. C., Mantz A., Barrett E., Henry J. P., Ma C. J., van Speybroeck L. 2010, MNRAS, 407, 83

Feretti L., Giovannini G., Govoni F., Murgia M. 2012, A&ARv, 20, 54
Hurley-Walker, N., *et al*. 2017, MNRAS 464, 1146
Intema H. T., van der Tol S., Cotton W. D., Cohen A. S., van Bemmel I. M., Röttgering H. J. A. 2009, A&A, 501, 1185
Intema H. T., Jagannathan P., Mooley K. P., Frail D. A. 2017, A&A, 598, A78
Mohan N., Rafferty D. 2015, ascl.soft, ascl:1502.007
Parekh V., Dwarakanath K. S., Kale R., Intema H. 2017, MNRAS, 464, 2752
Petrosian V. 2001, ApJ, 557, 560
Sandhu P., Malu S., Raja R., Datta A. 2018, Ap&SS, 361, 8
Scaife A. M. M., Heald G. H. 2012, MNRAS, 423, L30
Skillman, S. W., Xu, H., Hallman, E. J., *et al*. 2013, ApJ, 765, 21
Venturi T., Giacintucci S., Dallacasa D., Cassano R., Brunetti G., Bardelli S., Setti G. 2008, A&A, 484, 327
Wilson W. E., *et al*. 2011, MNRAS, 416, 832